



**HAL**  
open science

# Goal-Oriented Communications for Distributed Sensing: a joint scheduling and estimation approach

Maxime Ferreira Da Costa, Salah Eddine Elayoubi, Wassim Hajji

## ► To cite this version:

Maxime Ferreira Da Costa, Salah Eddine Elayoubi, Wassim Hajji. Goal-Oriented Communications for Distributed Sensing: a joint scheduling and estimation approach. IEEE 99th Vehicular Technology Conference, IEEE, Jun 2024, Singapore, Singapore. hal-04243611v2

**HAL Id: hal-04243611**

**<https://centralesupelec.hal.science/hal-04243611v2>**

Submitted on 22 Jul 2024

**HAL** is a multi-disciplinary open access archive for the deposit and dissemination of scientific research documents, whether they are published or not. The documents may come from teaching and research institutions in France or abroad, or from public or private research centers.

L'archive ouverte pluridisciplinaire **HAL**, est destinée au dépôt et à la diffusion de documents scientifiques de niveau recherche, publiés ou non, émanant des établissements d'enseignement et de recherche français ou étrangers, des laboratoires publics ou privés.

Copyright

# Goal-Oriented Communications for Distributed Sensing: a joint scheduling and estimation approach

Maxime Ferreira Da Costa, Salah Eddine Elayoubi, Wassim Hajji  
CentraleSupélec, Université Paris-Saclay, CNRS, L2S, Gif-sur-Yvette, France

**Abstract**—This paper tackles the problem of distributed sensing from a goal-oriented communications perspective. The case of sensors sampling sources in the environment and conveying the collected information to a fusion center over a wireless channel is considered. Herein, the objective of the communications is to achieve a reliable estimation of the sources, while preserving network resources. The fusion center task is formulated as a joint distributed sensing problem, where a scheduling policy has to be designed to optimize the applicative goal. Two distinct goals are considered: a) when the objective is to achieve the best possible estimation of the sources given a communication resource constraint; b) when the objective is to minimize the communication resource to estimate the sources up to a pre-determined precision. For both cases, the optimal scheduling policy is formulated as the solution to a constrained optimization problem. Greedy iterative algorithms are proposed to efficiently solve those problems for the particular case of independent sources. Numerical results illustrate the tradeoff between achievable estimation accuracy and resource consumption, and provide insights on the impact of the network structure on the achievable performance.

## I. INTRODUCTION

Goal-oriented communications have emerged as a novel paradigm in wireless networks. Goal is here tailored in terms of network performance at a specific application, rather than in terms of more classical telecommunication metrics such as the Quality of Service (QoS) or throughput. In other words, goal-oriented communications aim to maximize the impact of the received bits for a custom goal intended by the transmitter and the receiver [1]. It is sometimes called task-oriented, as in [2]. Goal-oriented communications have been identified as an enabler for sustainable networking, as only the necessary amount of data for achieving the goal is transmitted [3]. The first derivation of this paradigm focuses on point-to-point communication, where data is incoming from a single source. The case of real-time tracking of a source was considered in [4], and edge learning in [5]. Another context of application is the joint optimization of the network and application, which has been studied for image retrieval [6] or vehicle platooning controller design under channel imperfections [7].

While goal-oriented communications have gained significant interest in the past few years, the problem of distributed optimal sensing over wireless channels remains widely unexplored. We consider in this paper a scenario with distributed sampling and scheduling of information from multiple sources, observed by multiple sensors. Possible applications include collaborative computer vision, or joint localization of a target, where sensors acquire correlated signals that, once resolved together, provide

improved estimation of a statistical prior than the individual sensor estimates. The case where each sensor may have a partial view of the environment, with possibly overlapping observations, is considered. In order to derive the optimal sampling strategy, the network exploits its knowledge about the structure of the information retrieved from each sensor, and the radio conditions knowledge, *i.e.* the quality of the different wireless links between the sources and the 6G base station.

The proposed scenario relates partially to the framework of Integrated Sensing and Communications (ISAC). The ISAC mainstream of works integrates radar sensing and communications into the same hardware and spectrum, and uses the RF signals for sensing [8]. However, the broader concept of ISAC includes the cross-layer design of 5G/6G networks for conveying sensing information in an optimal way. To the best of our knowledge, this paper is the first to tackle the challenge of integrating sensing accuracy in radio resource allocation.

### A. Organization of the paper

Section II presents the system model, with sensors observing sources that might be correlated and conveying data over a wireless channel towards a fusion center for estimation. When the state of the environment is assumed to be Gaussian, the performance of the Minimum Mean Square estimator (MMSE) for the non-constrained case where all data are available at the fusion center is derived. Section III introduces the joint estimation and communication problem, where the communication resources are limited. Optimization techniques should be leveraged to discover the optimal sampling policy. The MMSE estimator for a given sampling policy (*i.e.* under incomplete data) is first derived, and the goal-oriented communication problem is formulated either in terms of minimizing the MMSE under communication constraints or in terms of minimizing the resource consumption for a target MMSE. Closed-form solutions are also derived for specific setups of interests. Section IV provides numerical experiments that illustrate the optimal policies for different joint sensing and scheduling settings, including the case of overlapped observation between sensors. A comparison is made between the studied goal-oriented schedulings and the classical “fair sampling” scheduling. A conclusion is drawn in Section V.

### B. Notations

The operators  $\text{var}$  and  $\text{cov}$  denote the variance of a random variable and the covariance between two random vectors,

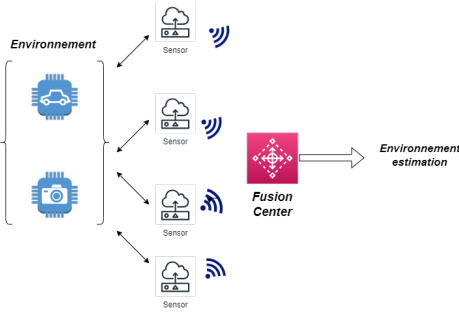


Figure 1. The distributed sensing model.

respectively. The matrix whose diagonal elements correspond to the elements of vector  $\mathbf{x}$  is written  $\text{diag}(\mathbf{x})$ .  $\text{Tr}(\mathbf{X})$  is the trace of matrix  $\mathbf{X}$ , and  $\mathbf{I}_k$  is the identity matrix in dimension  $k$ . We write  $\Pi_K = [0, 1]^K$  the hypercube in dimension  $K$ .

## II. SYSTEM MODEL

### A. Observation model

We consider  $K$  sources jointly monitoring an environment whose state  $\mathbf{s} \in \mathbb{R}^N$  is modeled as a random Gaussian vector with mean  $\boldsymbol{\mu}$  and covariance matrix  $\boldsymbol{\Sigma}$ :

$$\mathbf{s} = [s_1, \dots, s_N]^\top \in \mathbb{R}^N, \quad \mathbf{s} \sim \mathcal{N}(\boldsymbol{\mu}, \boldsymbol{\Sigma}). \quad (1)$$

At instant  $t$ , each sensor samples a partial measure of the state  $\mathbf{s}$ . A central entity, called *fusion center*, can query at each time instant the observation of some of the sensors over a wireless channel, according to its scheduling policy. At the end of the monitoring cycle, of duration  $T$ , the fusion center builds an estimate  $\hat{\mathbf{s}}$  of  $\mathbf{s}$ . It is assumed that each source observes a noisy linear form of the state leading to observation  $x_k$  sensor  $k$ :

$$x_k(t) = \langle \mathbf{a}_k, \mathbf{s} \rangle + e_k(t), \quad (2)$$

where  $\mathbf{a}_k \in \mathbb{R}^N$  is a sensing vector that is assumed to be known and  $e_k(t) \in \mathbb{R}$  is additive white Gaussian noise with 0 mean and variance  $\eta_k^2$ , that is  $e_k(t) \sim \mathcal{N}(0, \eta_k^2)$ . Overall, the observation is Gaussian with probability law

$$x_k(t) \sim \mathcal{N}(\mathbf{a}_k^\top \boldsymbol{\mu}, \mathbf{a}_k^\top \boldsymbol{\Sigma} \mathbf{a}_k + \eta_k^2), \quad (3)$$

and is correlated to both  $\mathbf{s}$  and  $e_k(t)$ . In the sequel, we derive the performance of the MMSE estimator of the state of the environment  $\mathbf{s}$ , first at the sensor level when estimation is done *individually*, and then at the fusion center when estimation is done *jointly* in the event of an *unconstrained* sampling policy where all sensors are queried at all time.

### B. Individual estimation at sensor level

We first consider the case of estimating  $\mathbf{s}$  from the acquisition of a single sensor during the whole cycle. To proceed, we assume the sensor computes the time average over the cycle  $y_k = \frac{1}{T} \sum_{t=0}^{T-1} x_k(t)$ . Under the measurement model (1) and (2), the MMSE estimator  $\hat{\mathbf{s}}_k$  of  $\mathbf{s}$  given  $y_k$  results of the Gaussian estimation formula (see e.g. [9, chapter 4]):

$$\hat{\mathbf{s}}_k = \text{cov}(\mathbf{s}; y_k) \text{var}(y_k)^{-1} y_k = \boldsymbol{\Sigma} \mathbf{a}_k \left( (\mathbf{a}_k^\top \boldsymbol{\Sigma} \mathbf{a}_k) + T^{-1} \eta_k^2 \right)^{-1} y_k \quad (4)$$

Moreover, this estimator achieves the MMSE:

$$\mathbb{E} \|\hat{\mathbf{s}}_k - \mathbf{s}\|_2^2 = \text{Tr} \left( \boldsymbol{\Sigma} - \left( (\mathbf{a}_k^\top \boldsymbol{\Sigma} \mathbf{a}_k) + T^{-1} \eta_k^2 \right)^{-1} \boldsymbol{\Sigma} \mathbf{a}_k^\top \mathbf{a}_k \boldsymbol{\Sigma} \right). \quad (5)$$

### C. Joint estimation with all sensors

We now turn to the case where all sensors collaborate for the estimation, and the fusion center combines the information of all sensors to estimate the sources. We define by  $\mathbf{x}(t) = [x_1(t), \dots, x_K(t)]^\top \in \mathbb{R}^K$  the joint observation vector at time  $t$ . From (2) we have that  $\mathbf{x}(t) = \mathbf{A}^\top \mathbf{s} + \mathbf{e}(t)$ , where  $\mathbf{A} = [\mathbf{a}_1, \dots, \mathbf{a}_K] \in \mathbb{R}^{N \times K}$  the sensing matrix of the system and  $\mathbf{e}(t) = [e_1(t), \dots, e_K(t)]^\top \in \mathbb{R}^K$  is the noise vector at time  $t$ . At the end of the sampling cycle, the fusion center computes

$$\mathbf{y} = \frac{1}{T} \sum_{t=0}^{T-1} \mathbf{A}^\top \mathbf{s} + \mathbf{e}(t), \quad (6)$$

and computes the MMSE estimate  $\hat{\mathbf{s}}$  the sources as

$$\begin{aligned} \hat{\mathbf{s}} &= \text{cov}(\mathbf{s}; \mathbf{y}) \text{cov}(\mathbf{y}; \mathbf{y})^{-1} \mathbf{y} \\ &= \boldsymbol{\Sigma} \mathbf{A} \left( \mathbf{A}^\top \boldsymbol{\Sigma} \mathbf{A} + T^{-1} \text{diag}(\boldsymbol{\eta}_k^2) \right)^{-1} \mathbf{y}, \end{aligned} \quad (7)$$

yielding the estimation error

$$\begin{aligned} \mathbb{E} \|\hat{\mathbf{s}} - \mathbf{s}\|_2^2 &= \\ &\text{Tr} \left( \boldsymbol{\Sigma} - \boldsymbol{\Sigma} \mathbf{A} \left( \mathbf{A}^\top \boldsymbol{\Sigma} \mathbf{A} + T^{-1} \text{diag}(\boldsymbol{\eta}_k^2) \right)^{-1} \mathbf{A}^\top \boldsymbol{\Sigma} \right). \end{aligned} \quad (8)$$

## III. JOINT SCHEDULING AND ESTIMATION POLICY

In this section is considered the joint estimation of the fusion center on the state of the environment  $\mathbf{s}$  when data acquisition is constrained by the network resources and the radio conditions of the links between each sensor and the fusion center. The channel between source  $k$  and the base station is assumed to be time-varying and differs from one source to another. This translates into a quantity of network resources  $r_k(t)$  to use to query the  $k$ -th source at time  $t$ . The parameter  $r_k(t)$  encompasses the packet length, the modulation scheme, and the realization of the  $k$ -th channel at time  $t$ <sup>1</sup>.

### A. Sampling process

A sampling policy of the base station consists of attributing a sampling frequency  $0 \leq \pi_k(t) \leq 1$  at time slot  $t \in [1, T]$  and for each source  $k$ . A realization of the policy consists of the subset of sources that are queried at time  $t$  by the base station. It is expressed by the vector  $\mathbf{f}(t) \in \{0, 1\}^K$  with component:

$$f_k(t) = \begin{cases} 1, & \text{with probability } \pi_k(t) \\ 0, & \text{with probability } 1 - \pi_k(t). \end{cases} \quad (9)$$

In the above the policy  $\pi_k(t)$  can be time-dependent. Herein, we restrict our analysis to the case where  $\pi_k(t)$  remains constant

<sup>1</sup>For instance, for a sensing packet of size  $g$  bits, a scheduling mini-slot of length  $\tau$ , a Resource Block (RB) of size  $w$  Hz, the resource consumption per packet of a sensor numbered  $k$  that is using a Modulation and Coding Scheme (MCS) of spectral efficiency  $e$  bit/s/Hz, is  $r_k = \frac{g}{w\tau e}$  RB per packet.

over a cycle duration, that is  $\pi_k(t) = \pi_k$  for  $0 \leq t \leq T - 1$ . Additionally,  $\mathbf{f}(t)$  and  $\mathbf{r}(t)$  are assumed to be independent random variables, meaning that the realizations of the sampling policy are independent of the realizations of the channel. However,  $\mathbf{f}(t)$  might depend on the channel statistics.

The average cost  $C(\boldsymbol{\pi})$  of the sampling the wireless sensors with the policy  $\boldsymbol{\pi}$  over a cycle is defined as:

$$C(\boldsymbol{\pi}) = \frac{1}{T} \mathbb{E} \left[ \sum_{t=0}^{T-1} \sum_{k=1}^K f_k(t) r_k(t) \right] = \sum_{k=1}^K \pi_k r_k \quad (10)$$

At the end of a cycle, the base station averages the samples acquired by each sensor into a vector  $\mathbf{z} \in \mathbb{R}^K$ , with entries  $z_k$  given by  $z_k = \frac{1}{T} \sum_{t=0}^{T-1} f_k(t) x_k(t)$ .

### B. MMSE estimator for a given policy

As the cycle length  $T$  increases, the random variable  $z_k$  will converge in law to a Gaussian random variable  $\tilde{z}_k$  that has the same distribution as the average of  $T \cdot \pi_k$  random variables each having the same distribution as  $x_k$ . Hence, the asymptotic behaviour  $\tilde{\mathbf{z}}$  of  $\mathbf{z}$  follows is drawn according to the multivariate Gaussian distribution

$$\tilde{\mathbf{z}} \sim \mathcal{N} \left( \text{diag}(\boldsymbol{\pi}) \mathbf{A}^\top \boldsymbol{\mu}, \text{diag}(\boldsymbol{\pi}) \mathbf{A}^\top \boldsymbol{\Sigma} \mathbf{A} \text{diag}(\boldsymbol{\pi}) + T^{-1} \text{diag}(\boldsymbol{\pi}) \text{diag}(\boldsymbol{\eta}^2) \right). \quad (11)$$

With that observation, we formulate an estimator of  $\hat{\mathbf{s}}_\pi$  from the observation  $\mathbf{z}$  under the sampling policy  $\boldsymbol{\pi}$  of the form

$$\begin{aligned} \hat{\mathbf{s}}_\pi &= \text{cov}(\mathbf{s}; \mathbf{z}) \text{cov}(\mathbf{z}; \mathbf{z})^{-1} \mathbf{z} \\ &= \boldsymbol{\Sigma} \mathbf{A} \text{diag}(\boldsymbol{\pi}) \left( \text{diag}(\boldsymbol{\pi}) (\mathbf{A}^\top \boldsymbol{\Sigma} \mathbf{A}) \text{diag}(\boldsymbol{\pi}) \right. \\ &\quad \left. + T^{-1} \text{diag}(\boldsymbol{\pi} \odot \boldsymbol{\eta}^2) \right)^{-1} \mathbf{z} \end{aligned} \quad (12)$$

When the cycle length  $T$  is large enough, the performance of  $\hat{\mathbf{s}}_\pi$  defined in (12) follows those of the Gaussian MMSE estimator, and the error covariance matrix  $\mathbf{K}$  is given by

$$\begin{aligned} \mathbf{K} &= \boldsymbol{\Sigma} - \text{cov}(\mathbf{s}, \mathbf{z}) \text{cov}(\mathbf{z}, \mathbf{z})^{-1} \text{cov}(\mathbf{s}, \mathbf{z})^\top \\ &= \boldsymbol{\Sigma} - \boldsymbol{\Sigma} \mathbf{A} \text{diag}(\boldsymbol{\pi}) \left( \text{diag}(\boldsymbol{\pi}) (\mathbf{A}^\top \boldsymbol{\Sigma} \mathbf{A}) \text{diag}(\boldsymbol{\pi}) \right. \\ &\quad \left. + T^{-1} \text{diag}(\boldsymbol{\pi} \odot \boldsymbol{\eta}^2) \right)^{-1} \text{diag}(\boldsymbol{\pi}) \mathbf{A}^\top \boldsymbol{\Sigma}^\top. \end{aligned} \quad (13)$$

For particular interest, the MSE is given by

$$\mathbb{E} \|\hat{\mathbf{s}}_\pi(\mathbf{z}) - \mathbf{s}\|_2^2 = \text{Tr}(\mathbf{K}). \quad (14)$$

In the sequel, we aim to understand the empirical properties of this estimator as a function of the policy  $\boldsymbol{\pi}$ .

*Remark:* When the sensor's observations are noiseless, *i.e.*  $\boldsymbol{\eta} = \mathbf{0}$ , the covariance of the MMSE estimator is independent of the sampling policy  $\boldsymbol{\pi}$  as long as every sensor is sampled at least once, *i.e.*  $\pi_k > 0$ . This property holds even when  $\mathbf{A}^\top \boldsymbol{\Sigma}$  is *not* full rank. In the latter case, the inverse in Equation (12) has to be replaced by its Moore–Penrose pseudo-inverse.

### C. Formulation as an optimization problem

In goal-oriented communication, the objective is to derive an optimal policy that takes into account both the estimation error on the state of the environment and the network resource consumption. To that end, we define two distinct optimization problems:

- *Performance maximization under communication constraint:* In this setting, the objective is to achieve the best applicative performance within an available budget of network resources. Given a resource budget  $R \geq 0$ , the optimal policy  $\boldsymbol{\pi}^*$  minimizes the objective

$$\boldsymbol{\pi}^* = \arg \min_{\boldsymbol{\pi} \in \Pi_K} \mathbb{E} \|\hat{\mathbf{s}}(\boldsymbol{\pi}) - \mathbf{s}\|_2^2 \quad \text{s.t.} \quad \sum_{k=1}^K \pi_k r_k \leq R. \quad (15)$$

- *Resource minimization under an applicative goal:* In this setting, the optimal policy  $\boldsymbol{\pi}^*$  is set to achieve a predetermined estimation error  $\varepsilon$  while minimizing resource consumption. It amounts to the optimization program

$$\boldsymbol{\pi}^* = \arg \min_{\boldsymbol{\pi} \in \Pi_K} \sum_{k=1}^K \pi_k r_k \quad \text{s.t.} \quad \mathbb{E} \|\hat{\mathbf{s}}(\boldsymbol{\pi}) - \mathbf{s}\|_2^2 \leq \varepsilon. \quad (16)$$

These two problems can be solved using the error expression in equation (14) with off-the-shelf solvers, and may lead to different scheduling policies, as will be seen next.

### D. Particular case of direct sampling of independent sources

This section considers the case where all  $K$  environment sources are directly and uniquely sampled by a sensor in the network. In this case,  $N = K$  and  $\mathbf{A} = \mathbf{I}_n$  is the identity matrix. Also, we assume independent sources of variances  $\sigma_n^2$  for  $n \in [1, N]$ . The MMSE of (14) reduces to:

$$\mathbb{E} \|\hat{\mathbf{s}}_\pi(\mathbf{z}) - \mathbf{s}\|_2^2 = \sum_{k=1}^K \frac{\sigma_k^2 \eta_k^2}{T \pi_k \sigma_k^2 + \eta_k^2} = \sum_{k=1}^K \frac{1}{T \pi_k \eta_k^{-2} + \sigma_k^{-2}} \quad (17)$$

- 1) *Performance maximization under communication constraint:* The optimization problem (15) become

$$\boldsymbol{\pi}^* = \arg \min_{\boldsymbol{\pi} \in \Pi_K} \sum_{k=1}^K \frac{1}{T \pi_k \eta_k^{-2} + \sigma_k^{-2}} \quad \text{s.t.} \quad \sum_{k=1}^K \pi_k r_k \leq R. \quad (18)$$

It is easy to show that the cost function to minimize is convex on  $\Pi_K$  as its Hessian is positive definite. Next, as the cost is strictly decreasing for  $\pi_k > 0$ , the constraint in To solve this problem, we first notice that the inequality constraint (18) is saturated at the optimum, that is  $\sum_{k=1}^K \pi_k^* r_k = R$ . The optimal policy  $\boldsymbol{\pi}^*$  can be retrieved from a Lagrangian analysis. The Lagrangian  $\mathcal{L}_1(\boldsymbol{\pi}, \lambda)$  of problem (18) writes

$$\mathcal{L}_1(\boldsymbol{\pi}, \lambda) = \sum_{k=1}^K \frac{1}{T \pi_k \eta_k^{-2} + \sigma_k^{-2}} + \lambda \left( \sum_{k=1}^K \pi_k r_k - R \right) \quad (19)$$

Setting the derivative with respect to  $\pi_k$  to 0 yields

$$\lambda = \frac{T\eta_k^{-2}}{r_k(T\pi_k\eta_k^{-2} + \sigma_k^{-2})^2}, \quad (20)$$

and the global solution to (18) writes

$$\pi_k^* = \left( \frac{R + \sum_{j=1}^N \frac{\eta_j^2 r_j}{T\sigma_j^2}}{\sqrt{\frac{\eta_k^2 r_k}{T}} \left( \sum_{j=1}^N \sqrt{\frac{\eta_j^2 r_j}{T}} \right)} - \frac{1}{\sigma_k^2} \right) \frac{\eta_k^2}{T} \quad (21a)$$

$$\lambda^* = \left( \frac{\sum_{j=1}^N \sqrt{\frac{r_k \eta_k^2}{T}}}{R + \sum_{j=1}^N \frac{r_k \eta_k^2}{T\sigma_k^2}} \right)^2. \quad (21b)$$

We note that  $\pi^*$  should be in the simplex  $\Pi_K$ . The solution (21) only meets this condition whenever the optimal dual variable  $\lambda^*$  takes value  $\lambda^* \in [\lambda_{\min}(k), \lambda_{\max}(k)]$  for  $k \in [1, N]$  with

$$\lambda_{\min}(k) := \frac{T\eta_k^{-2}}{r_k(T\eta_k^{-2} + \sigma_k^{-2})^2}; \quad \lambda_{\max}(k) := \frac{T\eta_k^{-2}}{r_k\sigma_k^{-4}}. \quad (22)$$

As the resource consumption  $\sum_{k=1}^K \pi_k r_k$  is increasing with the  $\pi_k$ , and the MMSE is decreasing with  $\pi_k$ . Suppose that the  $r_k$  are ranked in ascending order, we propose the following greedy iterative procedure to solve the problem:

- 1) Let  $k^\natural$  be the largest index such that  $\lambda^* < \lambda(k)$  with the convention  $k^\natural = 0$  if  $\lambda^* < \lambda(1)$ . Set  $\pi_k = 1$  for all  $k \leq k^\natural$ .
- 2) Let  $\underline{k}$  be the smallest index such that  $\lambda^* > \lambda_{\min}(k)$  with the convention  $\underline{k} = N + 1$  if  $\lambda^* > \lambda(N - 1)$ . Set  $\pi_k = 0$  for all  $k \geq \underline{k}$ .
- 3) For the other sources with indices  $k^\natural < k < \underline{k}$ , compute  $\pi_k$  by solving the intermediate optimization problem:

$$\begin{aligned} & \underset{\pi}{\text{minimize}} \quad \sum_{k=k^\natural+1}^{\underline{k}-1} \frac{1}{T\pi_k\eta_k^{-2} + \sigma_k^{-2}} \\ & \text{subject to} \quad \sum_{k=k^\natural+1}^{\underline{k}-1} \pi_k r_k \leq R - \sum_{j=1}^{k^\natural} r_j, \end{aligned} \quad (23)$$

whose solution is given by

$$\pi_k^* = \left( \frac{R - \sum_{j=1}^{k^\natural} r_j + \sum_{j=k^\natural+1}^{\underline{k}-1} \frac{\eta_j^2 r_j}{T\sigma_j^2}}{\sqrt{\frac{\eta_k^2 r_k}{T}} \left( \sum_{j=k^\natural+1}^{\underline{k}-1} \sqrt{\frac{\eta_j^2 r_j}{T}} \right)} - \frac{1}{\sigma_k^2} \right) \frac{\eta_k^2}{T}. \quad (24)$$

Here again, the solution of the modified algorithm may lead to values of  $\pi^*$  that are outside of the simplex  $\Pi_K$ . The heuristic algorithm should be repeated until narrowing the optimal solution to  $\Pi_K$ .

- 2) *Minimizing resource consumption for a given goal:*

We now move to problem (16). Under the hypothesis of Subsection III-D, the optimization problem becomes

$$\pi^* = \arg \min_{\pi \in \Pi_K} \sum_{k=1}^K \pi_k r_k \quad \text{s.t.} \quad \sum_{k=1}^K \frac{1}{T\pi_k\eta_k^{-2} + \sigma_k^{-2}} \leq \varepsilon \quad (25)$$

As in Subsection III-D1, the inequality constraint is saturated at the optimum, and the Lagrangian  $\mathcal{L}_2(\pi, \mu)$  of (25) is

$$\mathcal{L}_2(\pi, \mu) = \sum_k \pi_k r_k + \mu \left( \sum_{k=1}^K \frac{1}{T\pi_k\eta_k^{-2} + \sigma_k^{-2}} - \varepsilon \right) \quad (26)$$

The solution to this problem is

$$\pi_k = \frac{\eta_k^2}{T} \left( \sqrt{\frac{\mu^* T}{r_k \eta_k^2} - \sigma_k^{-2}} \right) \quad (27a)$$

$$\mu^* = \left( \frac{1}{\varepsilon} \sum_{j=1}^N \sqrt{\frac{r_k \eta_k^2}{T}} \right)^2. \quad (27b)$$

As before, this solution does not ensure that  $\pi \in \Pi_K$ . However, it is possible to follow a similar iterative greedy algorithm proposed in Subsection III-D1 to reach the optimal solution, by solving instead of (23) the intermediate optimization program

$$\begin{aligned} & \underset{\pi}{\text{minimize}} \quad \sum_{k=k^\natural+1}^{\underline{k}-1} \pi_k r_k \\ & \text{s.t.} \quad \sum_{k=k^\natural+1}^{\underline{k}-1} \frac{1}{T\pi_k\eta_k^{-2} + \sigma_k^{-2}} \leq \varepsilon - \sum_{j=1}^{k^\natural} \frac{1}{T\eta_j^{-2} + \sigma_j^{-2}} - \sum_{j=\underline{k}}^N \frac{1}{\sigma_j^{-2}}. \end{aligned} \quad (28)$$

#### IV. NUMERICAL EXPERIMENTS

In this section, a base station with  $N$  information sources is simulated, and the radio resource consumption is modeled according to the 5G NR Adaptive Modulation and Coding (AMC) table in [10, Table 5.2.2.1-4]. A classical FDD numerology with 15kHz subcarrier spacing and 2 OFDM symbols per mini-slot is considered. A sampling cycle consists of a slot (1 ms), and the sampling opportunities are based on a mini-slot basis, making  $T = 7$  mini-slots. As for the resource consumption model, we consider the practical case where the MCS is chosen at the beginning of the slot, so that  $r_k$  remains constant for the whole cycle, and might change from one slot to another.

##### A. Validation of the optimal policy

We first consider  $N = 4$  independent sources sampled directly with Channel Quality Indicator (CQI) indices (12, 10, 8, 6) (from [10, Table 5.2.2.1-4]). Every sampled packet has a size of 512 bits, leading to the resource consumption vector  $\mathbf{r} = (8, 11, 17, 33)$  RBs, using the spectral efficiencies of the aforementioned table.

We start by validating the algorithm for obtaining the optimal solution defined in Section III-D1. Figure 2 compares the optimal solution of (21) with the modified solution proposed by the greedy iterative method detailed in Subsection III-D1. While removing the simplex constraint  $\pi \in \Pi_K$  would lead to selecting sources with the best channel conditions with a sampling frequency greater than 1, the modified version forces these sampling frequencies to 1 and increases the sampling rate of other sources. Furthermore, it is shown that the modified solution matches the optimal one, obtained by directly solving the convex problem (21). Now, to estimate the accuracy of the

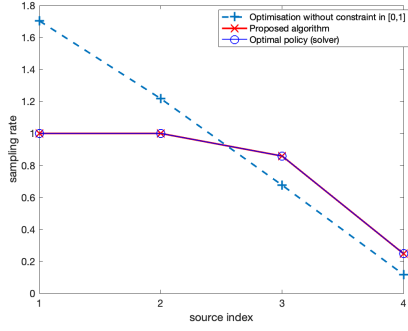


Figure 2. Illustration of the optimization algorithm ( $N = 4$ ,  $R = 40$  RBs).

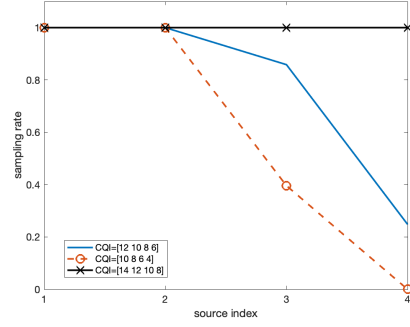


Figure 4. Impact of different channel conditions ( $N = 4$ ,  $R = 40$  RBs).

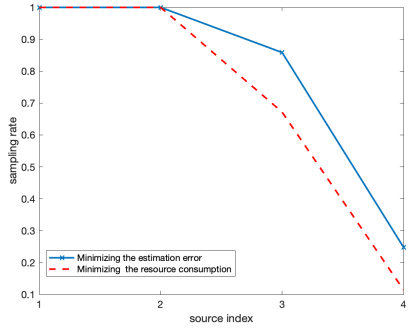


Figure 3. Maximizing accuracy vs; minimizing resource consumption.

optimal solution under the resource constraint, we compare the resulting MMSE with the one of a non constrained system (all sources are sampled all the time); the accuracy loss is 14%.

We now turn to the problem of minimal resource consumption under an error constraint as in Program (16). We set a target accuracy loss of 20% (instead of the 14% obtained with the optimal solution of Program (15) in Figure 2) and compare the optimal policies. In Figure 3, we observe lower sampling rates corresponding to an average resource consumption of 32 RBs, compared to the consumption of 40 RBs when the goal is set to minimize the estimation error.

### B. Sampling policy with varying CQI

We now study the impact of varying channel conditions on the policy. Figure 4 draws the optimal resource-constrained policies for three cases: when the CQIs are those used in Figure 2; when the CQIs are slightly smaller; and when the CQIs are slightly greater. We observe a large impact of the combination of the channel conditions, calling for adapting dynamically the sampling policy.

We thus simulate the system with changing wireless channels with time, leading to a different MCS for each cycle and a different subsequent resource consumption per sensor. In that scenario, the optimal policy varies with time. To illustrate the dynamic policy, we simulate the system where the sensors are deployed in fixed positions but with fluctuating channel CQIs and MCS, due to noise and interference. However, the average CQI remains better for sensors that are closer to the access

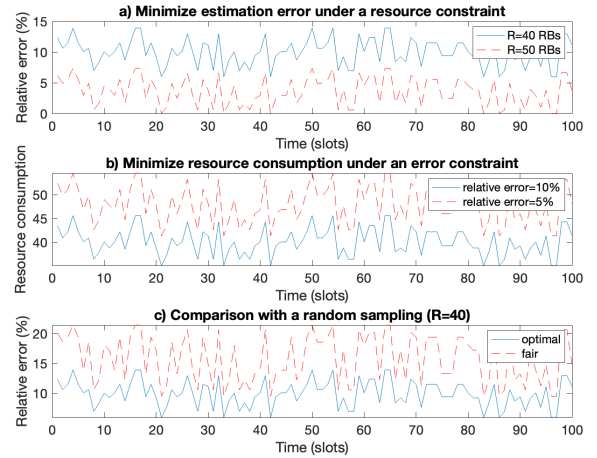


Figure 5. Performance evolution with changing radio condition.

point, and the instantaneous CQI varies around it following a uniform distribution. Figure 5 illustrates the performance of the dynamic policies when a) the estimation error is minimized when respecting a resource constraint; b) the average resource consumption for a constraint on the estimation error. The estimation error is defined as the relative difference between the MMSE for the given policy and the MMSE of the non-constrained policy. We observe that, for the case of a constraint on resources, the estimation error changes with time, but remains lower when more resources are available (for a larger  $R$ ). When the objective is to minimize resource consumption under a constraint on the relative error, the average amount of consumed resources increases when a tighter estimation constraint is set.

We also compare our scheme with a classical “fair” sampling scheme under a resource constraint  $R$ , where in the absence of information about the application performance, all sensors are sampled indiscriminately, that is  $\pi_k = \frac{R}{K}$ . Figure 5(c) compares the estimation error for the optimal scheme (the same as for figure 5-a with  $R = 40$ ) to this fair policy. A significant enhancement of the estimation error is observed for the goal-oriented approach.

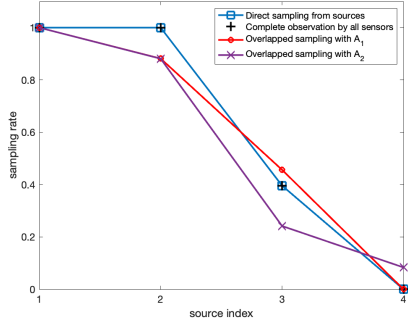


Figure 6. Impact of overlapped source observation ( $N = 4$ ,  $R = 40$  RBs,  $CQI=[10, 8, 6, 4]$ ).

### C. Sampling for sensors with overlapping

We now move to the more general case where sensors are decoupled from sources and may have overlapping observations. We assume independent observation errors of equal variance on each sensor, that is  $\eta_k^2 = \eta^2$  for all  $k \in [1, K]$ . Additionally, up to a rotation, we assume the entries  $s_n^*$  of the state of the environment to be uncorrelated with equal variance  $\sigma_n^2 = \sigma^2$  for all  $n \in [1, N]$ . The observation pattern is described by a matrix  $\mathbf{A}$ . The covariance matrix of equation (13) becomes

$$\mathbf{K} = \sigma^2 \mathbf{I}_n - \sigma^2 \mathbf{A} \text{diag}(\boldsymbol{\pi})$$

$$\left( \text{diag}(\boldsymbol{\pi}) \mathbf{A}^\top \mathbf{A} \text{diag}(\boldsymbol{\pi}) + T^{-1} \frac{\eta^2}{\sigma^2} \text{diag}(\boldsymbol{\pi}) \right)^{-1} \text{diag}(\boldsymbol{\pi}) \mathbf{A}^\top, \quad (29)$$

as in this case  $\boldsymbol{\Sigma} = \sigma^2 \mathbf{I}_n$  and  $\text{diag}(\boldsymbol{\pi} \odot \boldsymbol{\eta}^2) = \eta^2 \text{diag}(\boldsymbol{\pi})$ .

For the example, it is assumed scenarios with 4 sources and 4 sensors acting in four different observation patterns:

- 1) Each sensor observes one source, as in III-D.
- 2) Each sensor observes all sources ( $\mathbf{A}$  is a matrix of ones).
- 3) Sensors may observe multiple sources, with sensing matrices below. For matrix  $\mathbf{A}_1$ , sensors are assumed to observe two sources. For matrix  $\mathbf{A}_2$ , Sensors 1, 2, and 3 observe exactly one source, while the last one observes all sources with the worst radio conditions:

$$\mathbf{A}_1 = \begin{pmatrix} 1 & 0 & 0 & 1 \\ 1 & 1 & 0 & 0 \\ 0 & 1 & 1 & 0 \\ 0 & 0 & 1 & 1 \end{pmatrix}, \quad \mathbf{A}_2 = \begin{pmatrix} 1 & 0 & 0 & 1 \\ 0 & 1 & 0 & 1 \\ 0 & 0 & 1 & 1 \\ 0 & 0 & 0 & 1 \end{pmatrix}$$

We observe that the first two scenarios (one source per sensor and all sources observed by each sensor) lead to the same policy, as the situations are symmetrical. However, the later cases yield different solutions as the optimal policy specializes in the sampling pattern and the radio conditions. Furthermore, the experiment showcases the greater importance of sampling sensor 4 under observation pattern  $\mathbf{A}_2$ , as it is the only sensor providing information on the fourth environment state  $s_4$ .

## V. CONCLUSIONS

In this paper, we have developed a goal-oriented communications framework for distributed sensing in wireless

networks. The scenario consists of sensors observing sources and conveying their observations over a wireless channel to a data fusion center that estimates the sources. Instead of conveying all the generated data, we have proposed sampling and scheduling schemes that integrate the objective of the application into the decision. We have considered the minimization of the estimation error and the minimization of the resource consumption for selecting an optimal sampling policy and formulated two optimization problems. When directly sampling independent sources, iterative greedy procedures can be applied to calculate the optimal policy efficiently. Finally, we showcased the schemes for a distributed sensing problem in 5G NR. We showed how the observation structure and the radio conditions of sensors influence the optimal strategies. Numerical simulations highlight the benefits of adapting the sampling schemes over using a static ‘‘fair sampling’’ policy.

## ACKNOWLEDGMENT

This research work is supported by the Sustainable 6G research chair, held by CentraleSupélec, and funded by Orange.

## REFERENCES

- [1] E. C. Strinati and S. Barbarossa, ‘‘6G networks: Beyond shannon towards semantic and goal-oriented communications,’’ *Computer Networks*, vol. 190, p. 107930, 2021.
- [2] D. Gündüz, Z. Qin, I. E. Aguerri, *et al.*, ‘‘Beyond transmitting bits: Context, semantics, and task-oriented communications,’’ *IEEE Journal on Selected Areas in Communications*, vol. 41, no. 1, pp. 5–41, 2022.
- [3] S. E. Elayoubi and E. Hardouin, ‘‘For an energy sober network that contributes to a sustainable society,’’ in *IEEE Future Networks World Forum*, 2023.
- [4] N. Pappas and M. Kountouris, ‘‘Goal-oriented communication for real-time tracking in autonomous systems,’’ in *2021 IEEE International Conference on Autonomous Systems (ICAS)*, IEEE, 2021, pp. 1–5.
- [5] T.-Y. Tung, S. Kobus, J. P. Roig, and D. Gündüz, ‘‘Effective communications: A joint learning and communication framework for multi-agent reinforcement learning over noisy channels,’’ *IEEE Journal on Selected Areas in Communications*, vol. 39, no. 8, pp. 2590–2603, 2021.
- [6] M. Jankowski, D. Gündüz, and K. Mikołajczyk, ‘‘Wireless image retrieval at the edge,’’ *IEEE Journal on Selected Areas in Communications*, vol. 39, no. 1, pp. 89–100, 2020.
- [7] T. R. Gonçalves, V. S. Varma, and S. E. Elayoubi, ‘‘Relay-assisted platooning in wireless networks: A joint communication and control approach,’’ *IEEE Transactions on Vehicular Technology*, 2023.
- [8] F. Liu, Y. Cui, C. Masouros, *et al.*, ‘‘Integrated sensing and communications: Toward dual-functional wireless networks for 6G and beyond,’’ *IEEE journal on selected areas in communications*, vol. 40, no. 6, pp. 1728–1767, 2022.
- [9] S. P. Boyd and L. Vandenberghe, *Convex optimization*. Cambridge university press, 2004.
- [10] ‘‘5G; NR; Physical layer procedures for data, TS 38.214 version 16.5.0 Release 16,’’ 3GPP, Tech. Rep., Apr. 2021.